Journal of Superconductivity and Novel Magnetism (2020) 33:3107–3112
https://doi.org/10.1007/s10948-020-05558-3

ORIGINAL PAPER

Prediction of Half-Metallic Ferromagnetism in Cu- and K-Doped MgS: A Comparative Study

W. Adli[1]

Received: 2 May 2020 / Accepted: 28 May 2020 / Published online: 12 June 2020

Abstract
Ab initio calculations based on density functional theory have been used to comparatively investigate the electronic and magnetic properties of two non-magnetic ions (Cu, K)-doped magnesium sulfide. The results obtained indicate that the ferromagnetic phase is always energetically favorable than the paramagnetic one. It is also found that these ternary alloys are half-metallic ferromagnets with a total magnetic moment of 1.00 μ_B per supercell. The ferromagnetism is induced by hybridization between Cu *3d* and its nearest neighboring S *3p* in Cu-doped MgS, while it originates in the spin polarization of the *p* shell of anions S in K-doped MgS. Our results make these compounds attractive materials for possible spintronics devices.

Keywords Diluted magnetic semiconductor · Half-metallic ferromagnetism · *p-d* hybridization · *p*-electron ferromagnetism

1 Introduction

Diluted magnetic semiconductors (DMSs) have been extensively studied due to their potential applications in the field of spintronics [1–3]. In particular, half metallic DMSs are attracting a considerable amount of attention, for which only one of the two spin channels presents a gap at the Fermi level (E_F), while the other has a metallic character, leading 100% carrier spin polarization at E_F. For practical microelectronic device applications, half metallic (HM) ferromagnets should exhibit ferromagnetism at room or higher temperatures [4]. During the past years, significant research efforts have been made toward studying the room temperature ferromagnetism in transition metal (TM)-doped II–VI and III–V semiconductors [5–13]. However, the origin of ferromagnetism in these alloys continues to be a subject of debate. This is because the TM-doped semiconductors usually suffer from the problems of the precipitates or secondary phase formation [14, 15]. To avoid these controversies, many research works have been focused on investigating the ferromagnetism of the intrinsic nonmagnetic element-doped semiconductors, such as Cu-doped ZnO [16, 17], GaN [18], and AlN [19, 20]. Besides Cu, other intrinsic nonmagnetic elements, like K, C, and Sr, can also lead to ferromagnetism in AlN [21], ZnO [22, 23], and III–V [24], respectively. More interestingly, most of these studies indicate the possibility of fabricating the room temperature ferromagnets, which provide an opportunity to study new mechanisms of ferromagnetism and open new ways to find advanced spintronic materials.

Due to their wide band gaps and low dielectric constants, the magnesium chalcogenides, MgX (X = S, Se, and Te) have received enormous interest from both experimental and theoretical points of view. These semiconductors can be used in blue and ultraviolet wavelength optics and high temperature electronics [25–27]. Among magnesium chalcogenides, magnesium sulfide (MgS) has a very large band gap, in excess of 4.5 eV, and it is an excellent barrier material with most other II–VI semiconductors [28]. MgS exists in abundance in the earth's crust [29]; it crystallizes in the rock-salt structure as ground state under ambient pressure [30]. In addition, the zinc blende structure is realized by means of epitaxial growth over GaAs substrate either by metallo-organic vapor phase epitaxy (MOVPE) [31, 32] or by molecular beam epitaxy (MBE) [33]. Although many theoretical and experimental reports have been carried out for MgS, only few works have reported on the magnetism of MgS-based DMS. Liu et al. [34] using pseudopotential method have predicted the presence of the character half-metallic in C-doped alkaline earth chalcogenides X_4CY_4 (X = Mg, Ca, and Sr, Y = O and S) with NaCl structure.

✉ W. Adli
Adli.phys@gmail.com

[1] Département de Génie Physique, Faculté de Physique, Université des Sciences et de la Technologie d'Oran (USTO), BP 1505 El-M'naouer, 31000 Oran, Algeria

Table 1 Predicted equilibrium lattice constant a (Å), bulk modulus B (Gpa), its pressure derivative for both paramagnetic (PM) and ferromagnetic (FM) phases, and total energy difference ΔE (meV/cell) of $Mg_{1-x5}Cu_xS$ and $Mg_{1-x}K_xS$

Compounds	a (Å)		B (Gpa)		B'		ΔE (meV)
	FM	PM	FM	PM	FM	PM	
$Mg_{0.75}Cu_{0.25}S$	5.623	5.620	59.092	59.321	4.237	4.363	20.62
$Mg_{0.875}Cu_{0.125}S$	5.667	5.664	56.399	57.754	3.940	3.976	47.85
$Mg_{0.9375}Cu_{0.0625}S$	5.689	5.690	55.731	55.686	4.725	4.229	55.63
$Mg_{0.75}K_{0.25}S$	6.021	6.020	39.751	40.557	4.652	5.088	72.58
$Mg_{0.875}K_{0.125}S$	5.860	5.858	46.238	47.243	4.158	3.683	87.86
$Mg_{0.9375}K_{0.0625}S$	5.782	5.781	51.075	51.045	4.022	4.045	48.51

In the present work, the influence of K and Cu as nonmagnetic dopants on the half-metallicity and electronic structure of zinc blende MgS is examined by first principle calculations. The theoretical analysis of the electronic structures provides us a clear understanding of the governing mechanisms behind K and Cu dopant-induced HM ferromagnetism. The paper is organized as follows. In Section 2, we briefly describe our method of calculation. Section 3 contains all results and discussions. Finally, we conclude with a summary in Section 4.

2 Method

To perform the calculations, we have employed the full potential of linear augmented plane wave method within the density functional theory (DFT) [35], as implemented in the wien2K package [36]. We considered different compositions, namely 25%, 12.5%, and 6.25% which correspond to supercell containing 8, 16, and 32 atoms, respectively, for $Mg_{1-x}Cu_xS$ and $Mg_{1-x}K_xS$ systems. The generalized gradient approximation (GGA) proposed by Perdew, Burke, and Ernzerhof (PBE) [37] is used to treat the exchange and correlation functional. The basis function was expanded to R_{MT} $K_{max} = 8$, where R_{MT} is the muffin-tin radius and K_{max} is the maximum modulus for the reciprocal lattice vectors. The maximum value of partial waves inside the atomic sphere is l = 10. Full relativistic approximation is used for core electrons, and scalar relativistic approximation is used for valence electrons. Muffin-tin radii (R_{MT}) of 2 bohr are chosen for all atoms. Brillouin zone integrations are performed using 5 × 5 × 5 k-points of Monkhorst-Pack [38] (MP) mesh for the supercell calculations. During calculations, the atomic coordinates are fully relaxed until maximum force on a single atom is less than 2.10^{-3} Ry/a.u., and convergence of energy is set at 10^{-5} Ry/cell.

3 Results and Discussions

To explore the ground state properties, we first optimize the total energy as function of cell volume of studied DMS compounds for both ferromagnetic (FM) and paramagnetic (PM) phases. The calculated total energies are fitted with Murnaghan's equation of state [39]. The optimized lattice parameter, bulk modulus, its pressure derivative, and total energy difference ΔE between PM and FM states at their equilibrium lattice constants are tabulated in Table 1. In all cases, the FM phase is favorable in energy than the corresponding PM phase.

Table 2 shows the calculated magnetic properties of the studied alloys at their optimized equilibrium lattice constants for various concentrations of dopants. For all investigated compounds, the total magnetic moment is exactly $1.00\mu_B$. An integer value of magnetic moment is a characteristic feature of half-metallic ferromagnetism. The total magnetic moment m^{total} in supercell consists mainly of the following three parts: the $m^{Cu/K}$, m^S, and $m^{interstitial}$; however, the m^{Mg} is found

Table 2 Magnetic moments of the whole supercell, of the Cu/K site, of the nearest neighboring S site, of Mg site, and of interstitial regions

Compounds	$m^{interstitial}(\mu_B)$	$m^{Mg}(\mu_B)$	$m^{Cu/K}(\mu_B)$	$m^S(\mu_B)$	$m^{total}(\mu_B)$
$Mg_{0.75}Cu_{0.25}S$	0.228	0.002	0.400	0.094	1.00
$Mg_{0.875}Cu_{0.125}S$	0.231	0.001	0.394	0.089	1.00
$Mg_{0.9375}Cu_{0.0625}S$	0.230	0.001	0.402	0.072	1.00
$Mg_{0.75}K_{0.25}S$	0.388	−0.002	0.016	0.150	1.00
$Mg_{0.875}K_{0.125}S$	0.381	−0.001	0.020	0.148	1.00
$Mg_{0.9375}K_{0.0625}S$	0.388	0.001	0.013	0.105	1.00

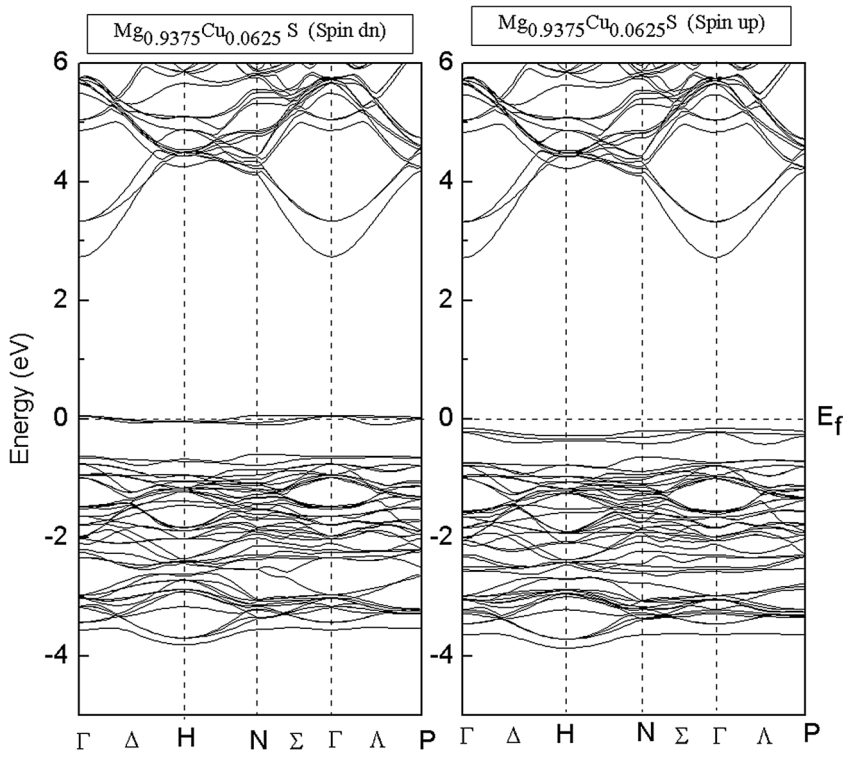

Fig. 1 The spin-resolved band structure of MgS doped with 6.25% of Cu. The left represents the minority spin band structure, and the right represents the majority spin band structure. Fermi level is set to 0.0 eV

negligible. For $x = 0.0625$, the magnetic moments are mainly localized within the Cu/K atom and its four nearest neighboring S atoms with the m^{Cu} (m^{K}) is larger (smaller) than that of the S atoms. The magnetic moments on other S atoms away from $(Cu/K)S_4$ tetrahedron are weak and not listed in Table 2.

As the trends in $Mg_{1-x}Y_xS$ (Y = Cu and K) alloys at different doping compositions are similar, in the following, we focus the discussion on the properties of doped ternary $Mg_{0.9375}Y_{0.0625}S$ systems at the equilibrium lattice parameters. Figures 1 and 2 present the spin-dependent band

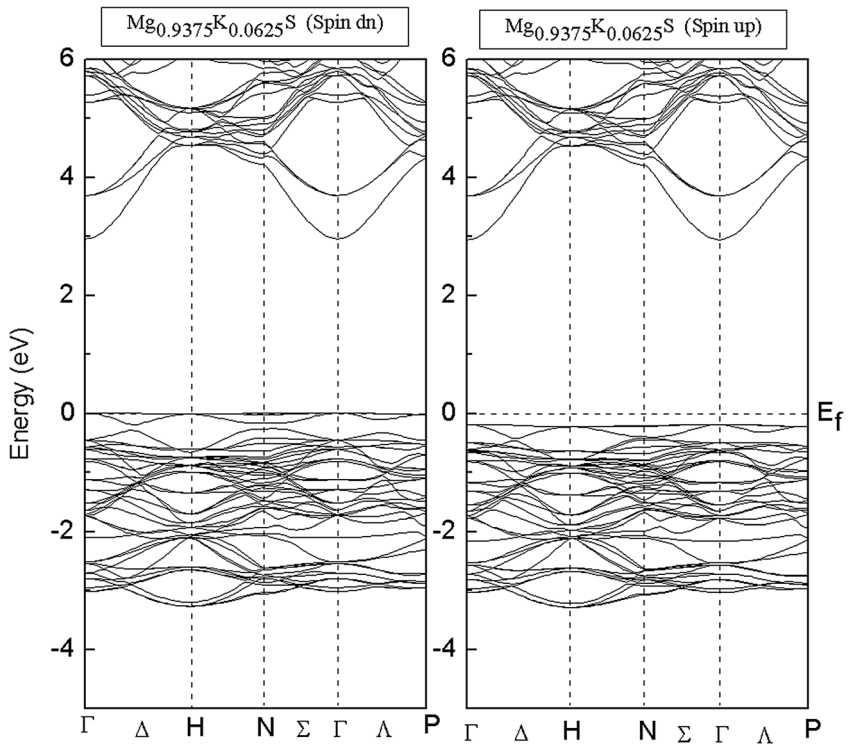

Fig. 2 The spin-resolved band structure of MgS doped with 6.25% of K. The left represents the minority spin band structure, and the right represents the majority spin band structure. Fermi level is set to 0.0 eV

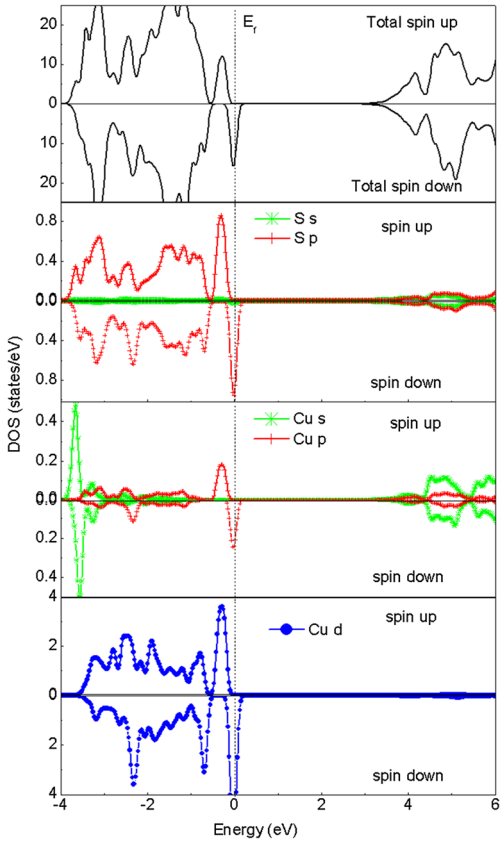

Fig. 3 (Color online) Total and partial density of states of MgS doped with 6.25% of Cu. The upper (lower) panel corresponds to the majority (minority) spin. The dashed vertical line indicates the Fermi level at 0.0 eV

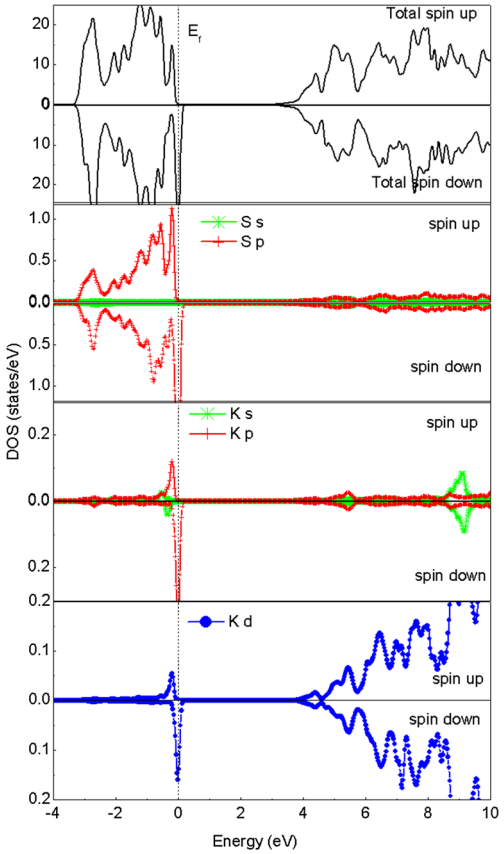

Fig. 5 (Color online) Total and partial density of states of MgS doped with 6.25% of K. The upper (lower) panel corresponds to the majority (minority) spin. The dashed vertical line indicates the Fermi level at 0.0 eV

structures along the high symmetry directions of the Brillouin zone for each compound. The band structures of both materials show half-metallic behavior. The minority spin electrons exhibit metallic natures, while the majority spin channels display a band gap of 2.88 eV for MgCuS and 3.13 eV for MgKS, revealing their semiconducting natures. The carriers are thus 100% polarized, which is the ideal case for spin injection applications. For MgKS, near the Fermi levels, there is a flat (undispersed) band in the whole Brillouin zone for both spin channels. This flat band is formed mainly from the S *3p* orbitals. For the sake of comparison of magnetism mechanisms in Y-doped MgS DMS, we first analyze the total density of states (DOS) and partial DOS of Cu and its one nearest neighboring S for MgCuS. As can been seen in Fig. 3, the asymmetrical DOS between the spin up and spin down channels near the Fermi level (E_F) shows the magnetic properties

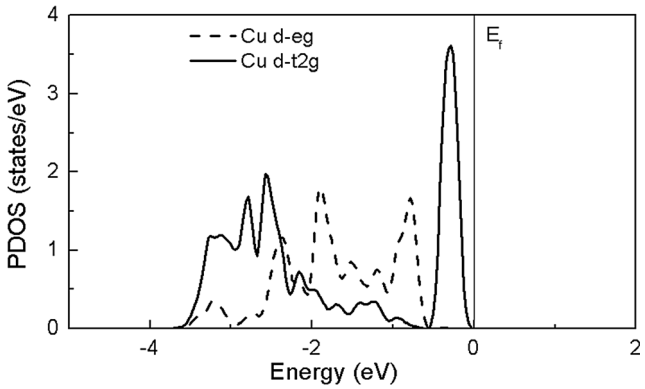

Fig. 4 Cu *3d* projected partial density of state (PDOS) of MgS doped with 6.25% of Cu for the majority spin. The solid vertical line denotes the position of the Fermi level

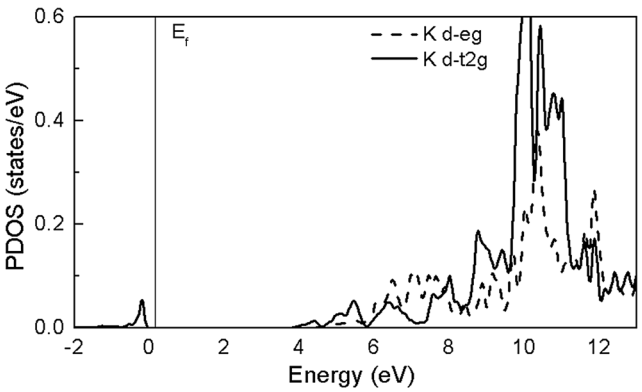

Fig. 6 K *3d* projected partial density of state (PDOS) of MgS doped with 6.25% of K for the majority spin

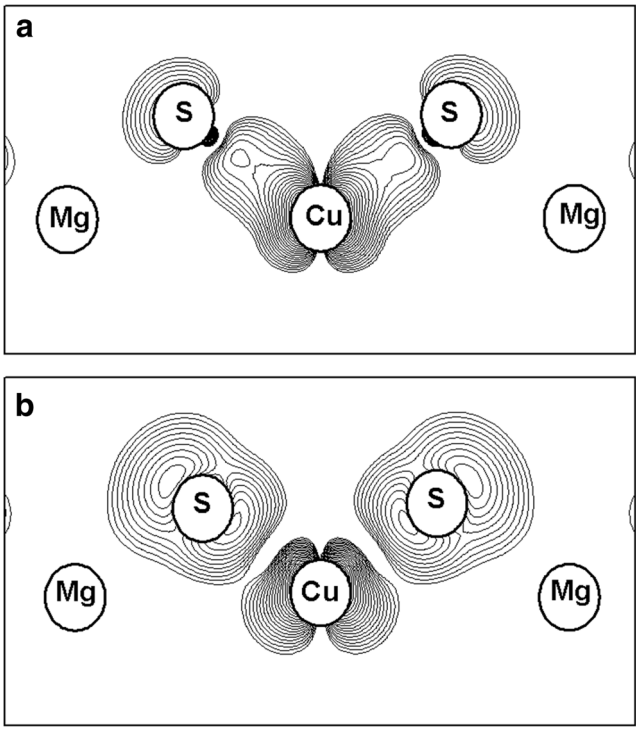

Fig. 7 Partial spin-up valence charge density of $Mg_{0.9375}Cu_{0.0625}S$ within CuS_4 tetrahedron at Γ point in (110) plane. (**a**) Energy at − 2.55 eV and (**b**) energy at − 0.23 eV

of such doped system. The density of states between − 4 and − 0.6 eV is mostly ascribed to the Cu *d* and S *p* states with relatively small contribution of Cu *s* and Cu *p* states. States around E_F arise primarily from the Cu *3d* orbitals, hybridized strongly with S *3p* orbitals. The character of dominating states at and near E_F can be elucidated by crystal field theory, in which the cation *d* states are split into triply degenerate t_{2g} and doubly degenerate e_g states, whereas the anion *p* states transform as t_{2p} representation. The states with the same t_2 symmetry for spin up (or spin down) between the anion and cation can couple with each other forming lower bonding and higher antibonding states, known as the *p-d* coupling, while the e_g states cannot bond by symmetry and do not take part in the hybridization process. The contribution of these symmetry

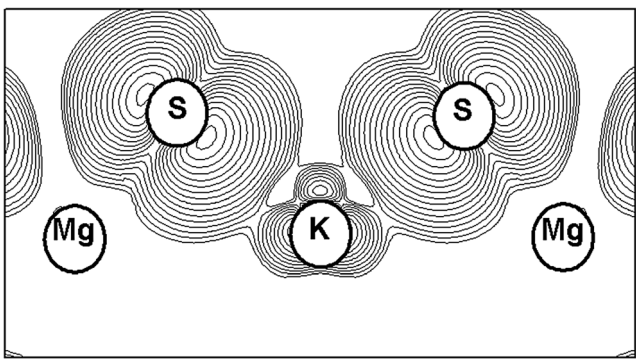

Fig. 8 Partial spin-up valence charge density of $Mg_{0.9375}K_{0.0625}S$ within KS_4 tetrahedron at Γ point in (110) plane at around − 0.18 eV

states toward total spin-up DOS is shown in Fig. 4. Therefore, the induced S t_2 states can couple only Cu t_{2g} states having the same symmetry. Consequently, the *p-d* coupling mechanism is responsible for the HM ferromagnetism in this compound.

Having discussed the origin of ferromagnetism in MgCuS, we now turn our attention to the MgKS compound. The spin-resolved total and partial density of state of MgKS are given in Fig. 5. It reveals that the anionic and cationic states contribute differently to the majority spin system. The states ranging from − 1 eV and E_F are mainly composed of S *3p* states with a slight contribution from K *3p* and K *3d* states. However, there is a K *s* peak at − 0.52 eV, which is different from TM-doped MgS [40, 41]. Also, from the DOS, a sharp peak is found at the top of the valence states. The Fermi level is located at the peak of minority spin states, i.e., in the gap of the majority spin states. One can clearly see that the peak of the DOS can be attributed to the almost dispersionless flat band shown in Fig. 2. It has been argued by other authors [42, 43] that the origin of this flat band is an interference effect between cationic t_{2g}-character and anionic *p*-character and that the flat band is essential for HM ferromagnetism. In the present case, these conditions are fulfilled (Figs. 5 and 6). However, most t_{2g} states are not occupied and lie at higher energies, and thus, K *d* splitting does not play an important role in FM K-doped MgS. The spin splitting mainly originates from S *p* states and is situated close to E_F, which provides the main magnetic moment, and the hybridization between S *p* and K *p* and K t_{2g} states leads to the small magnetic moment of the K atom. This is consistent with the results obtained in NaN and KN [44] and Sr-doped III–V [24] from first principle calculations.

The general picture of ferromagnetism that applies to MgCuS and MgKS systems can also be viewed in the charge density contour of spin up at the Γ point in Fig. 7 and Fig. 8, respectively. The fully filled majority spin at around − 2.55 eV are bonding Cu (t_{2g})-S(*p*) states, reflecting the covalent *p-d* bonding (i.e., the density lobes point toward the nearest neighbors, see Fig. 7a), while the antibonding Cu (t_{2g})-S(*p*) states are close to E_F (i.e., the density lobes point between the nearest neighbor atoms, see Fig. 7b). The occupied states of MgKS close to the E_F are strongly localized around the S atom, reflecting the weak polarized covalent bonds of S p orbitals and K electrons.

4 Summary

We have employed the first principle calculation to investigate the electronic and magnetic properties of $Mg_{1-x}Y_xS$ (Y = K, Cu) alloys for $x = 0.0625$, 0.125 and x = 0.25 in their ordered zinc blende structure. We found that the structure within ferromagnetic configuration is always the stable ground state. All doped ternary systems exhibit half metallic character with a

band gap for the majority spin channel and a partially filled band for the minority spin channel. It was observed that the total magnetization is 1.00 μ_B per dopant atom, and it remains independent on the dopant content. Also, it is revealed by means of partial DOS that the *p-d* coupling between cation and its neighboring anions plays a crucial role in forming the ferromagnetism Cu-doped MgS, while for K-doped MgS, the magnetism owns its origin to the spin polarization of S *p* states. With no magnetic element in these ternary alloys and the 100% spin polarization of the carriers, we expect Cu- and K-doped MgS to be promising half-metallic DMSs free from magnetic precipitates.

References

1. Ohno, H.: Science. **281**, 951 (1998)
2. Wolf, S.A., Awschalom, D.D., Buhrman, R.A., Daughton, J.M., von Molnar, S., Roukes, M.L., Chtchelkanova, A.Y., Treger, D.M.: Science. **294**, 1488 (2001)
3. Cui, X.Y., Medvedeva, J.E., Delley, B., Freeman, A.J., Stampfl, C.: Phys. Rev. B. **78**, 245317 (2008)
4. Jungwirth, T., Sinova, J., Masek, J., Kucera, J., MacDonald, A.H.: Rev. Mod. Phys. **78**, 809 (2006)
5. Liu, C., Yun, F., Morkoç, H.: J. Mater. Sci. Mater. Electron. **16**, 555 (2005)
6. Pearton, S.J., Norton, D.P., Ip, K., Heo, Y.W., Steiner, T.: J. Vac. Sci. Technol. B. **22**, 932 (2004)
7. Akhtar, M.S., Malik, M.A., Riaz, S., Naseem, S.: Mater. Chem. Phys. **160**, 440 (2015)
8. Kumar, D., Antifakos, J., Blamire, M.G., Barber, Z.H.: Appl. Phys. Lett. **84**, 5004 (2004)
9. Frazier, R.M., Thaler, G.T., Leifer, J.Y., Hite, J.K., Gila, B.P., Abernathy, C.R., Pearton, S.J.: Appl. Phys. Lett. **86**, 052101 (2005)
10. Dhar, S., Brandt, O., Trampert, A., Däweritz, L., Friedland, K.J., Ploog, K.H., Keller, J., Beschoten, B., Güntherodt, G.: Appl. Phys. Lett. **82**, 2077 (2003)
11. Chitta, V.A., Coaquira, J.A.H., Fernandez, J.R.L., Duarte, C.A., Leite, J.R., Schikora, D., As, D.J., Lischka, K., Abramof, E.: Appl. Phys. Lett. **85**, 3777 (2004)
12. Granville, S., Ruck, B.J., Preston, A.R.H., Stewart, T., Budde, F., Trodahl, H.J., Bittar, A., Downes, J.E., Ridgway, M.: J. Appl. Phys. **104**, 103710 (2008)
13. Zhi, Z.Y., Chun, H.M.: Chin. Phys. Lett. **21**, 1632 (2004)
14. Park, J.H., Kim, M.G., Jang, H.M., Ryu, S., Kim, Y.M.: Appl. Phys. Lett. **84**, 1338 (2004)
15. Kaspar, T.C., Droubay, T., Heald, S.M., Engelhard, M.H., Nachimuthu, P., Chambers, S.A.: Phys. Rev. B. **77**(R), 201303 (2008)
16. Ye, L.-H., Freeman, A.J., Delley, B.: Phys. Rev. B. **73**, 033203 (2006)
17. Buchholz, D.B., Chang, R.P.H., Song, J.-Y., Ketterson, J.B.: Appl. Phys. Lett. **87**, 082504 (2005)
18. Wu, R.Q., Peng, G.W., Liu, L., Feng, Y.P., Huang, Z.G., Wu, Q.Y.: Appl. Phys. Lett. **89**, 062505 (2006)
19. Ran, F.Y., Subramanian, M., Tanemura, M., Hayashi, Y., Hihara, T.: Appl. Phys. Lett. **95**, 112111 (2009)
20. Jia, W., Han, P., Chi, M., Dang, S., Xu, B., Liu, X.: J. Appl. Phys. **101**, 113918 (2007)
21. Han, R., Yuan, W., Yang, H., Du, X., Yan, Y., Jin, H.: J. Magn. Magn. Mater. **326**, 45 (2013)
22. Pan, H., Yi, J.B., Shen, L., Wu, R.Q., Yang, J.H., Lin, J.Y., Feng, Y.P., Ding, J., Van, L.H., Yin, J.H.: Phys. Rev. Lett. **99**, 127201 (2007)
23. Zhou, S., Xu, Q., Potzger, K., Talut, G., Grötzschel, R., Fassbender, J., Vinnichenko, M., Grenzer, J., Helm, M., Hochmuth, H., Lorenz, M., Grundmann, M., Schmidt, H.: Appl. Phys. Lett. **93**, 232507 (2008)
24. Adli, W.: J. Supercond. Nov. Magn. **30**, 1775 (2017)
25. Okuyama, H., Nakano, K., Miyajima, T., Akimoto, K.: Jpn. J. Appl. Phys. **30**, L1620 (1991)
26. Wang, M.W., Phillips, M.C., Swenberg, J.F., Yu, E.T., McCaldin, J.O., McGill, T.C.: J. Appl. Phys. **73**, 4660 (1993)
27. Wang, M.W., Swenberg, J.F., Phillips, M.C., Yu, E.T., McCaldin, J.O., Grant, R.W., McGill, T.C.: Appl. Phys. Lett. **64**, 3455 (1994)
28. Wang, M., Li, X., Gao, M., Pan, H., Liu, Y.: J. Alloys Compd. **603**, 158 (2014)
29. Sanchez, A.M., Olvera, J., Ben, T., Morrod, J.K., Prior, K.A., Molina, S.I.: Appl. Phys. Lett. **89**, 121907 (2006)
30. Peiris, S.M., Campbell, A.J., Heinz, D.L.: J. Phys. Chem. Solids. **55**, 413 (1994)
31. Uesugi, K., Obinata, T., Suemune, I., Kumano, H., Nakahara, J.: Appl. Phys. Lett. **68**, 844 (1996)
32. Konczewicz, L., Bigenwald, P., Cloitre, T., Chibane, M., Ricou, R., Testud, P., Briot, O., Aulombard, R.L.: J. Cryst. Growth. **159**, 117 (1996)
33. Bradford, C., O'Donnell, C.B., Urbaszek, B., Balocchi, A., Morhain, C., Prior, K.A., Cavenett, B.C.: Appl. Phys. Lett. **76**, 3929 (2000)
34. Liu, J., Chen, L., Dong, H.-N., Zheng, R.-L.: Appl. Phys. Lett. **95**, 132502 (2009)
35. Hohenberg, P., Kohn, W.: Phys. Rev. B. **136**, B864 (1964)
36. Blaha, P., Schwarz, K., Madsen, G.K.H., Kvasnicka, D., Luitz, J.: WIEN2k, an Augmented Plane Wave Program for Calculating Crystal Properties. Vienna University of Technology, Vienna (2001)
37. Perdew, J.P., Burke, K., Ernzerhof, M.: Phys. Rev. Lett. **77**, 3865 (1996)
38. Monkhorst, H.J., Pack, J.D.: Phys. Rev. B. **13**, 5188 (1976)
39. Murnaghan, F.D.: Proc. Natl. Acad. Sci. U. S. A. **30**, 244 (1944)
40. Gous, M.H., Meddour, A., Bourouis, C.: J. Magn. Magn. Mater. **422**, 271 (2017)
41. Tanveer, W., Mahmood, Q., Faridi, M.A., Yaseen, M., Ramay, S.M., Mahmood, A.: J. Supercond. Nov. Magn. **30**, 3481 (2017)
42. Yao, K.L., Jiang, J.L., Liu, Z.L., Gao, G.Y.: Phys. Lett. A. **359**, 326 (2006)
43. Sieberer, M., Redinger, J., Khmelevskyi, S., Mohn, P.: Phys. Rev. B. **73**, 024404 (2006)
44. Zhang, Y., Qi, Y., Hu, Y.: J. Magn. Magn. Mater. **324**, 2523 (2012)